Int. J. Electrochem. Sci., 13 **(2018)** 11895 – 11905, doi: 10.20964/2018.12.26

International Journal of ELECTROCHEMICAL SCIENCE
www.electrochemsci.org

Short Communication

Electrochemical stability of Titanium-Hydroxyapatite implantable material modified with Ceftriaxone

Luiza Ichim, Cristian Pîrvu, Claudiu Constantin Manole[*]

Politehnica University of Bucharest, Faculty of Applied Chemistry and Materials Science, Str. Gheorghe POLIZU, nr. 1-7, sector 1, 011061, Bucharest, Romania
[*]E-mail: claudiu.manole@upb.ro

Received: 13 March 2018 / *Accepted:* 15 May 2018 / *Published:* 5 November 2018

Operating room infections are a cause for concern when dealing with post-operation recovery. The main topic of this study is to observe the influence of drug release on electrochemical stability over time. This is achieved by applying a ceftriaxone antibiotic coating on the surface of a bioinspired implant. Surface analysis was made using FT-IR analysis and the X-Ray diffraction (XRD) technique. Electrochemical impedance spectroscopy (EIS) and potentiodynamic polarization were used to study the behavior of our sample in a normal saline solution. Drug release over time was also investigated using UV-VIS spectrophotometry.

Keywords: titanium, hydroxyapatite, ceftriaxone salt, electrochemical impedance spectroscopy

1. INTRODUCTION

Titanium is the preferred metal when considering implantable devices, especially the ones which involve long-term use [1]. This is mainly due to its strong protection against corrosion combined with compatible mechanical performance [2,3].

Titanium develops a native passive stratum which is formed simply by exposure to air. The passive oxide film formed over the metal inhibits metal dissolution. This occurs at the cost of decreased ionic conductivity through the passive film [4]. An annealing process in the oxygen atmosphere further enhances the stability of the metal by the formation of crystalline oxide at the metal interface, leading to a considerable reduction in surface defects [5]. In turn, this is coupled with a decrease in ion diffusion within the oxide film, [6] thus meaning that the material is more bioinert from a biological perspective [7]. In order to address this issue, hydroxyapatite is deposited to make the titanium more bioactive [8]. This hydroxyapatite deposition aids the biological integration process of the implantable titanium [9]. Furthermore, the hydroxyapatite layer provides a reported increase in the corrosion resistance of the commercially pure titanium [10].

When considering medical device implantation (such as a spinal implant or other orthopedic implants), the success of such an operation can be determined by two main factors: the formation of surface biofilm; and immune activity at the implant interface with the body [11]. Hydroxyapatite, as a major natural, inorganic component of the bone structure, facilitates the biofilm formation on the surface [12]. With respect to immune activity, the local release of an antibiotic substance leads to an improvement in the immune response [13]. The purpose of this paper is to monitor the electrochemical stability of the antibiotic-covered Titanium/Hydroxyapatite and correlate this stability with the antibiotic release. Due to its prolonged half-life, Ceftriaxone (as sodium salt) is chosen in this paper as the antibiotic [14]. Nevertheless, the electrochemical procedure presented herein can also be applied to similar antibiotics.

2. MATERIALS AND METHODS

2.1 Materials

Medical grade NaCl 0.9 % was used as provided by SC Infomed Fluids SRL. Ceftriaxone sodium salt (commercial name Cefort), containing 1g Ceftriaxone, was purchased from Antibiotice SA. Ceftriaxone sodium salt was diluted by using 10 ml of ultrapure water as a solvent. The solution was freshly prepared and used for deposition on the Ti plate on which hydroxyapatite (HA) was previously formed.

2.2 Electrodeposition of Ti sample with HA

A three electrode configuration consisting of Ag/AgCl as reference electrodes was used for the electrochemical experiments. The electrolytic growth solution contained 9.91 g/L $Ca(NO_3)_2$ x $4H_2O$ and 2,875 g/L $NH_4H_2PO_4$ purchased from Sigma Aldrich. A platinum bar served as a counter electrode while the Ti sample served as the working electrode. The electrodeposition transient, HA, on titanium plates was registered using a Volta Master 40 Potentiostat. The Ti/HA sample was annealed for 1h at 400 degrees.

2.3 Electrochemical deposition of Ceftriaxone on Ti/HA sample

The drug coating was produced by using the Autolab PGStat 302N with the chronoamperometry method for 90 s, applying a constant potential of 0,16V vs. open circuit potential. The typical three-electrode electrochemical cell was used with the Ti/HA sample substrate as working electrode, a Pt wire as counter electrode, and a standard Ag/AgCl as reference electrode. The solution deposition contained 2 g of Ceftriaxone salt dissolved in 20 ml of ultrapure water. After the electrochemical deposition of the coatings, samples were rinsed with distilled water and dried at room

temperature. The obtained samples were characterized using electrochemical impedance spectroscopy and Tafel analysis. The Autolab PGStat 302N was used in the same three-electrode configuration mentioned above.

2.4 Electrochemical characterization

The electrochemical experiments were made in a NaCl 0.9% electrolyte with Autolab PGStat 302N in the same three-electrode configuration. The linear polarization experiments were made between –0.25 V and 0.25 V vs OCP with a scan rate of 1 mV/s and a step potential of 1 mV. The Electrochemical Impedance Spectroscopy (EIS) was done at a frequency range between 100 kHz and 0.1 Hz with an amplitude of 10 mV. The samples were left immersed in the electrolyte for various periods of time (1 minute to 2 hours). The characterizations were made after each immersion time.

2.5 Spectroscopic and structural characterization

In order to obtain a release dosage [15] for Ceftriaxone, the calibration curve was obtained using a Perkin Elmer Lambda 900 UV-VIS spectrophotometer.

Subsequently, the ceftriaxone-loaded samples were immersed in the NaCl 0.9% solution. After certain immersion times of the ceftriaxone samples (from 1 min to 2 hours), the concentration in the solution was obtained using the previously-determined calibration curve.

The experimental data acquisitions were achieved by using the UVWinLab 5.2.0.0646 software, and the surface characterization was made using a FT-IR with the spectral range of 4000–400 cm^{-1} with a Perkin-Elmer Spectrum, USA.

The images in Figure 1 were processed with Chimera [16] and the chemical formula of Ceftriaxone from ChemSpider [17] while the hydroxyapatite crystal was reproduced afterwards [18].

Nanocomposite samples were investigated using X-ray powder diffraction (XRD) on the D8 DISCOVER diffractometer with Cu K_α radiation (λ=1.5406A), Gobell speculum, and the Lynx Eye OD detector. The measurement involved a 0.04^0 increment, a scan speed of 3 s/pas and a tangential incidence angle (theta) of 1^0.

3. RESULTS AND DISCUSSION

Ceftriaxone Sodium is an antibiotic used to treat a wide range of bacterial infections. It is included on the List of Essential Medicines drafted by the World Health Organization [19]. Due to a negatively charged region (highlighted in Figure 1 a), it presents electrophilic attraction onto positively charged species. This allows the use of electrochemical techniques for depositing the antibiotic onto metal implants. Next to the deposition aspects, there is a control means requirement for the formation

and adsorption of Ti/hydroxyapatite (Ti/HA), and for the release of ceftriaxone. Both are detailed in this section.

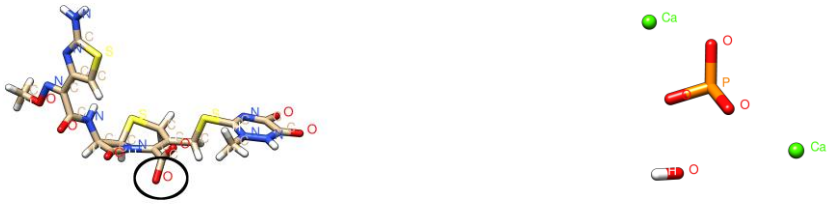

a) b)

Figure 1. Chemical formula of a) ceftriaxone antibiotic with the negative O^- group highlighted; and b) a hydroxyapatite crystal.

3.1. Hydroxiapatite surface characterization

The Hydroxyapatite coating was confirmed using the XRD technique. The phases have been identified using the Powder Diffraction File database from the International Center for Diffraction Data (ICDD).

The XRD results in Figure 2 show the hydroxyapatite peak contribution at 2θ = 32, 33 and 49 in accordance with the ASTM F 1185-88 standard [20]. The average size of crystallite was calculated with the Debye-Scherer equation at 119.6 Å, and with the phase on [2 1 2] direction. The hydroxyapatite film is 60.3 % crystalline after thermal treatment [21].

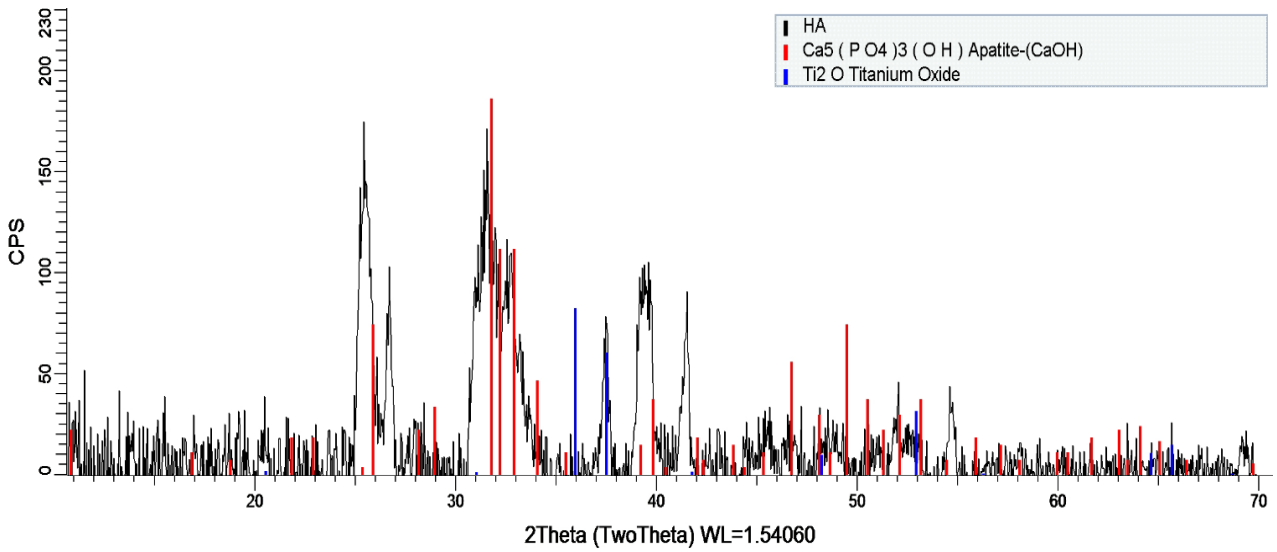

Figure 2. X-ray Diffraction pattern for titanium substrate coated in hydroxyapatite.

3.2. Ceftriaxone deposition on the titanium/hydroxyapatite interface

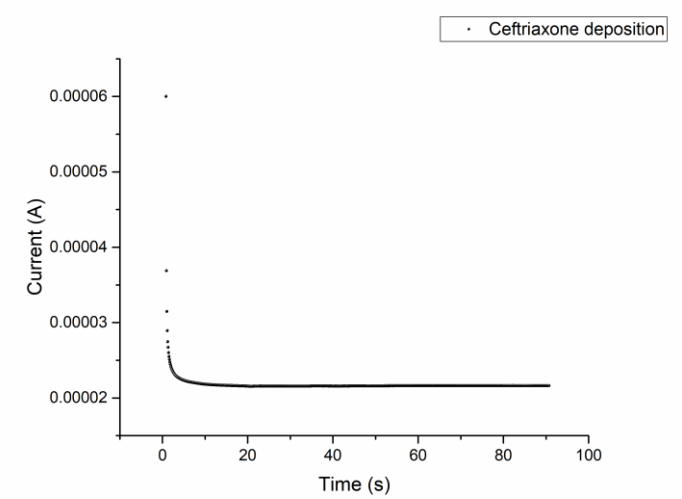

Figure 3. Electrochemical deposition of Ceftriaxone on Ti/HA sample; CFX was deposited at an applied potential of 0.16 V vs OCP.

Hydroxyapatite (HA) is a mineral with a chemical formula of $Ca_5(PO_4)_3(OH)$ (Figure 1 b). The aspects of the HA electrochemical deposition on the titanium plate are consistent with the previous results [22]. After thermal treatment, the titanium (Ti/HA) covered in hydroxyapatite is prepared for antibiotic deposition.

Ceftriaxone, as previously mentioned, possesses a negative CO^- terminal region (Figure 1 b) and can thus be attracted to positively charged surfaces. Chronoamperometry is the electrochemical tool used to follow the deposition kinetics on the Ti/HA (Figure 3).

3.3. Analysis of sample structures

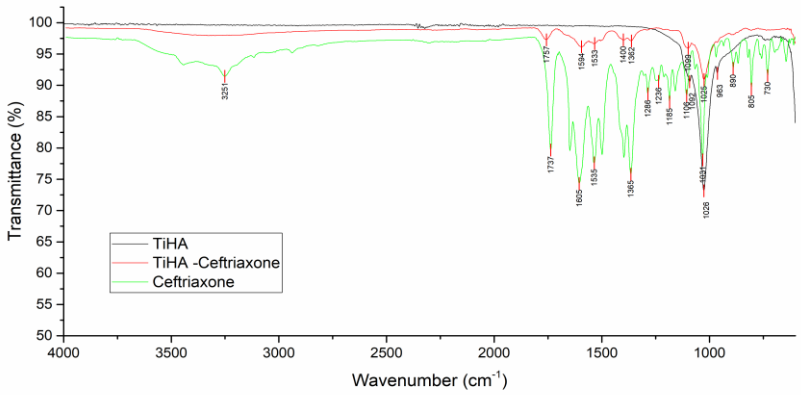

Figure 4. The FTIR spectra for the ceftriaxone powder and the titanium/hydroxyapatite(Ti/HA) covered in ceftriaxone. Peak regions are highlighted with contributions from ceftriaxone and both ceftriaxone and hydroxyapatite.

The ceftriaxone deposition on Ti/HA and Ti/HA/Ceftriaxone is confirmed by FTIR data. The referenced spectra are presented in Figure 4.

The stretching and wagging vibrations of the PO_4^{3-} group were observed around the bands of 986 cm^{-1} and 1056 cm^{-1}. The bands at around 3474 cm^{-1} correspond to the OH^- bands. The stretching vibration of the carbonate band was noticed at 1646 cm^{-1}[12]. These spectra confirmed the apatite formation phase in all coatings.

In the 1800 cm^{-1} – 1200 cm^{-1} region, the ceftriaxone-specific peaks highlight the deposition on the Ti/HA surface. In the 1200 cm^{-1} - 900 cm^{-1} range, there is a superposition of the ceftriaxone peaks on those of the hydroxyapatite mineral.

3.4. Electrochemical behavior of TiO_2/HA/Ceftriaxone samples with different immersion time in NaCl 0.9% solution

The metallic / electrolytic biomaterial interface was characterized using the Electrochemical Impedance Measurement (EIS) and was measured for its open circuit potential. Figure 5 and Figure 6 present the results of the EIS, represented in a Nyquist diagram and a Bode plot.

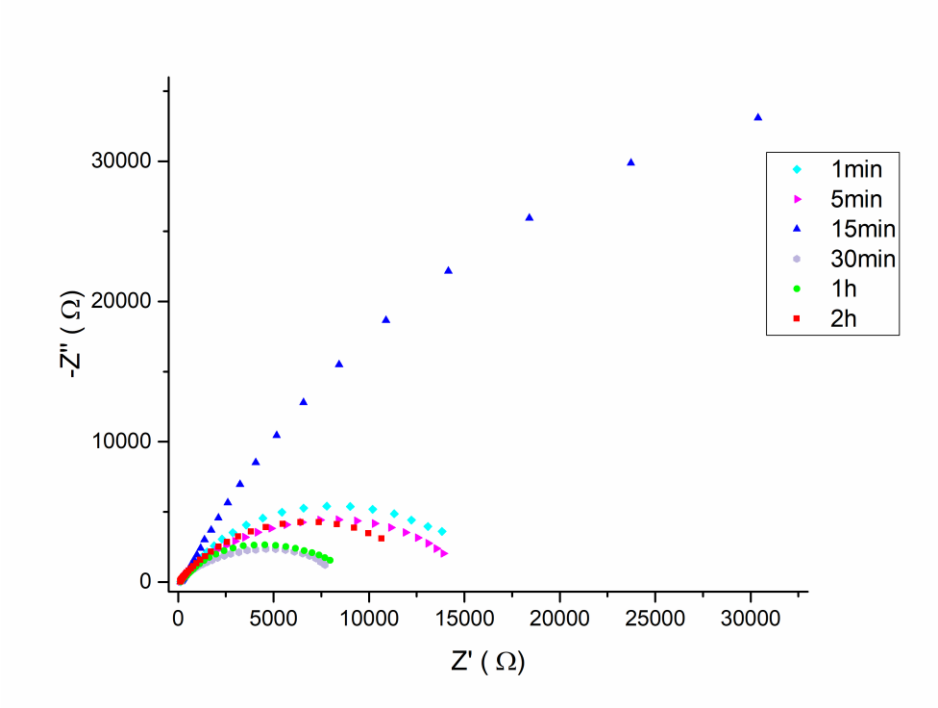

Figure 5. Nyquist diagrams for Ti/HA/ Ceftriaxone samples with different immersion time in NaCl 0.9% solution; during the experiments, an electronic oscillation of 10 mV was applied at an interval of 100 kHz to 0.1 Hz.

From the Nyquist diagrams, it is clear that all samples indicate the characteristics of a semicircle. It was found that the Debye semicircle has a larger diameter on the sample immersed for 15 min in saline solution, indicating a higher value of resistance to polarization.

These results are consistent with potentiodynamic polarization measurements, and they strengthen the 15 min mark as a key moment in Ceftriaxone release.

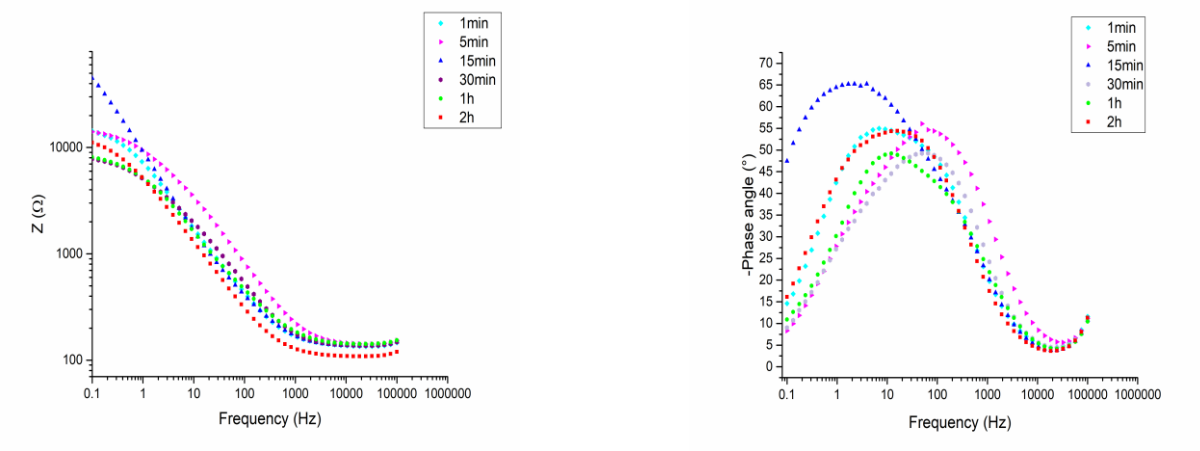

a) b)

Figure 6. Bode plots a) and b) for Ti/HA/ Ceftriaxone samples with different immersion time in NaCl 0.9% solution; during the experiments, an electronic oscillation of 10 mV was applied at an interval of 100 kHz to 0.1 Hz.

From the Bode plots, the phase angle for all materials noticeably decreases to zero degrees at very high frequencies, indicating that the solution-specific resistance dominates the impedance at this frequency range. In the low frequency range, the phase angle can be noticed dropping significantly, demonstrating that the impedance is active only as the resistance of the film is being formed on the surface of the material. This behavior is consistent for the presence of a thin oxide film on the surface of the studied samples.

Table 1. Parameters obtained from the EIS fitting data.

Immersion time (min)	***R_s* (Ω)**	***R_{ct}* (kΩ)**	***CPE_{ct}***		***R_{ox}* (kΩ)**	***CPE_{ox}***	
			***Q_{ct}* (µMho)**	***n_{ct}***		***Q_{ox}* (µMho)**	***n_{ox}***
1	130	1.21	170.00	1.00	15	31.80	0.70
5	132	2.76	17.50	0.76	12	23.30	0.75
15	133	1.50	156.00	0.58	100	25.80	0.83
30	129	7.02	44.30	0.72	1.4	26.90	0.77
60	137	8.81	33.50	0.70	0.05	14.20	0.98
120	105	12.80	41.90	0.75	0.32	104.00	0.80

The obtained parameters of the electric circuit components are shown in Table 1. With respect to the n_{ox}, the oxide layer parameters behave fairly similarly with the Ti/HA layers under various electrochemical setups [24].

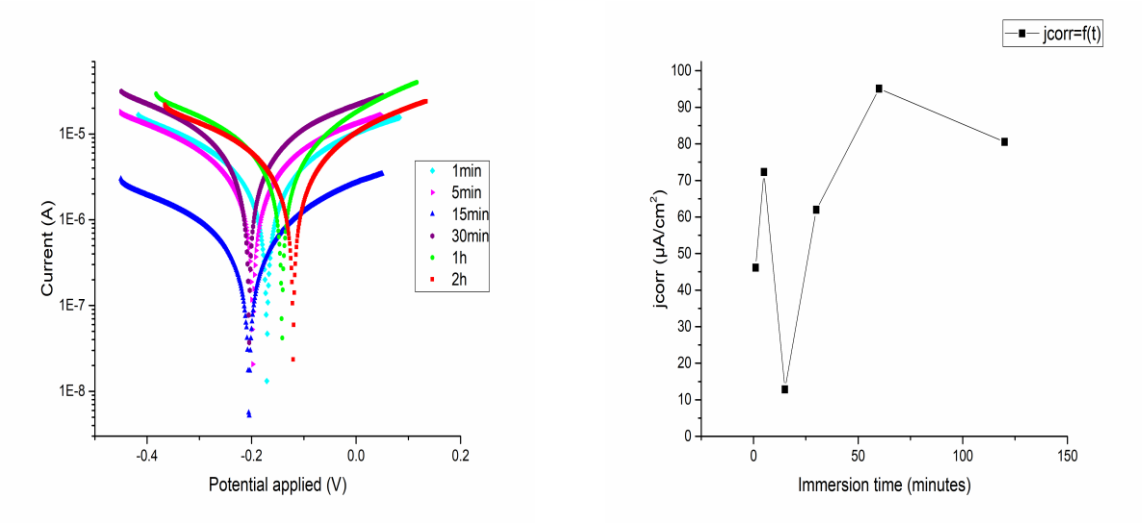

a) b)

Figure 7. a) Polarization curves for Ti/HA/ Ceftriaxone samples for different periods of time in NaCl 0.9% solution; b) corrosion current (j_{corr}) variation with different immersion time —the experiments were made at -0.25 V and + 0.25 V vs OCP range with a scan rate of 1 mV/s and a step potential of 1 mV.

The presence of charged Ceftriaxone on the surface in the first minute is confirmed by the capacitive behavior of n_{ct} = 1. At 15 min, there is a predominant behavior towards diffusion at n_{ct} = 0.58.

The numerical data is obtained after the results of the EIS experiment. R_s, R_{ct}, and R_{ox} represent the solution resistance, charge transfer and oxide layer respectively. Q_{ct} and Q_{ox} represent the admittances for the charge transfer and oxide layer respectively, and the n_{ct} and n_{ox} represent the constant phase element for the charge transfer and oxide layer respectively.

The polarization curves for the samples immersed in saline solution at varying immersion times are presented in Figure 7. The corresponding values obtained after a Tafel fit for the corrosion potential (E_{corr}), corrosion current (j_{corr}), polarization resistance and corrosion rate (expressed in μm/year) are presented in Table 2. According to these values, the polarization resistance value in the NaCl 0.9% solution is observed to be higher for Ti/HA/CFX at a 15-min immersion when compared to the rest of the samples.

Based on a study of the literature, an alloy that has a tendency towards passivity will have a b_a value greater than b_c, while a corroded alloy will have a b_a value lower than b_c [23]. By comparing the

values of the b_a to b_c in all samples, we can say that the corrosion processes taking place on the surface are under anodic control. This control implies the existence of a stable, passive layer on the surface of the material. Furthermore, the apparent, obtained results are brought about by the Ceftriaxone release in the NaCl solution, highlighted most strikingly with highest polarization resistance at 15 min.

Table 2. The electrochemical parameters obtained by extrapolation of Tafel curves for all materials coated in a saline solution.

Immersion time	E_{corr} **(mV)**	j_{corr} **(µA/cm^2)**	b_a **(mV/dec)**	b_c **(mV/dec)**	***Corrosion rate*** **(µm/year)**	R_{pol} **(kΩ)**
1 min	-170	46.15	413	410	0.40	17.14
5 min	-197	72.30	608	547	0.63	15.31
15min	-205	12.84	729	498	0.11	91.57
30 min	-206	61.96	321	282	0.54	9.32
1 h	-141	95.09	558	401	0.83	9.47
2 h	-120	80.55	643	460	0.70	12.79

To investigate whether or not the polarization curves indeed reflect the release of Ceftriaxone in the electrolyte, a study of its release is done using spectroscopic methods in similar conditions.

3.5. Ceftriaxone release behavior on TiO_2/HA/ Ceftriaxone samples in a NaCl 0.9% solution

Using Lambert-Beer, an extinction value of ε = 42.55 mL mg^{-1} cm^{-1} was obtained for the molar absorptivity of the Ceftriaxone [25]. Based on this data, the release rate was observed at key moments in time, as represented in Table 3.

Table 3. Ceftriaxone salt release quantity based on UV-VIS measurements.

Time (min)	1	5	15	30	60	120
Ceftriaxone Quantity (mg)	0.30	0.73	1.35	1.33	1.31	1.29

From Table 3, we notice the release of the largest quantity of Ceftriaxone in a 0.9% NaCl solution at 15 min. This confirms the electrochemical behavior and indicates two main steps of Ceftriaxone release: a) a fast release corresponding to the physical absorption of the drug, followed by b) a steady release [15].

The release behavior contains considerable importance with respect to pharmacokinetics, but also when considering that some surgical implantations (such as the typical hip replacement surgery) take around 1-2 hours to be performed.

4. CONCLUSIONS

In this study, Ceftriaxone salt was incorporated through an electrochemical deposition in Ti/HA biomaterials. The sample composition was investigated using FTIR and XRD analysis. Experiment data from the Tafel plots demonstrates a higher value of Ti/HA/ Ceftriaxone polarization resistance at 15 min of immersion when compared with the rest of the samples.

From the Nyquist diagrams, we observed that our results are consistent with the potentiodynamic polarization measurements, further strengthening the 15 min mark as a key moment in Ceftriaxone release.

A capacitive behavior of n_{ct} = 1 is attributed to charged Ceftriaxone on the surface in the first min. At 15 min, there is a predominant behavior towards diffusion at n_{ct} = 0.58.

In the final section, the antibiotic release had been studied. The sample immersed in saline solution for 15 min had a higher value of polarization resistance. We can correlate the behavior of the previously mentioned sample with the ceftriaxone release time (15 min).

ACKNOWLEDGEMENTS
The work has been funded by the Sectorial Operational Programme Human Resources Development 2007-2013 of the Ministry of European Funds through the Financial Agreement POSDRU/159/1.5/S/134398. We thank Beatrice Gabriela SBARCEA from the National Institute for R&D in Electrical Engineering ICPE-CA Bucharest for the XRD results.

References

1. D.M. Brunette, P. Tengvall, M. Textor and P. Thomsen, Titanium in Medicine: Material Science, Surface Science, Engineering, Biological Responses and Medical Applications, Springer Science & Business Media, (2011) Springer-Verlag Editorial/Production Heidelberger Platz 3 D-14197, Berlin.
2. D.C. Hansen, *Electrochem. Soc. Interface,* 17 (2008) 31.
3. M. Andreiotelli, H.J. Wenz and R.-J. Kohal, *Clin. Oral Implants Res*., 4 (2009) 32.
4. N.D. Tomashov, G.P. Chernova, Y.S. Ruscol, G.A. Ayuyan, *Electrochimica Acta,* 19 (1974) 159.
5. W. Ma, Z. Lu and M. Zhang*, Appl. Phys. Mater. Sci. Process.,* 66 (1998) 621.
6. L. Kavan, M. Grätzel, S.E. Gilbert, C. Klemenz and H.J. Scheel, *J. Am. Chem. Soc.,* 118 (1996) 6716.
7. M. Xiao, Y.M. Chen, M.N. Biao, X.D. Zhang and B.C. Yang, *Mater. Sci. Eng. C.,* 70 (2017) 1057.
8. D. Ionita, D. Bajenaru Georgescu and M. Prodana, *Rev. Chim. (Bucharest),* 67 (2016) 297.
9. L. Le Guéhennec, A. Soueidan, P. Layrolle and Y. Amouriq, *Dent. Mater.*, 23 (2007) 844.

10. A. Anawati, H. Tanigawa, H. Asoh, T. Ohno, M. Kubota and S. Ono, *Corros. Sci.*, 70 (2013) 212.
11. S.B. Goodman, Z. Yao, M. Keeney and F. Yang, *Biomaterials*, 34 (2013) 3174.
12. M. Prodana, M. Duta, D. Ionita, D. Bojin, M. S. Stan**,** A. Dinischiotu and I. Demetrescu, *Ceram. Int.*, 41 (2015) 6318.
13. S.L. Henry and K.P. Galloway, *Clin. Pharmacokinet.*, 29 (1995) 36.
14. G.M. Joynt, J. Lipman, C.D. Gomersall, R.J. Young, E.L.Y. Wong and T. Gin, *J. Antimicrob. Chemother.*, 47 (2001) 421.
15. D. Ionita, D. Bajenaru-Georgescu, G. Totea, A. Mazare, P. Schmuki and I. Demetrescu, *Int. J. Pharm.*, 517 (2017) 296.
16. H.E. Pence and A. Williams, *J. Chem. Educ.*, 87 (2010) 1123.
17. R.M. Wilson, J.C. Elliott and S.E.P. Dowker, *Am. Mineral*, 84 (1999) 1406.
18. E.F. Pettersen, T.D. Goddard, C.C. Huang, G.S. Couch, D.M. Greenblatt, E.C. Meng and T.E. Ferrin, *J. Comput. Chem*., 25 (2004) 1605.
19. World Health Organization, WHO model list of essential medicines: 19th list. http://apps.who.int/iris/handle/10665/70640.
20. G.Willmann, *Biomed. Tech.* (Berl), 35 (1990) 205.
21. D. Covaciu Romonți, G. Voicu and M. Prodana, *Int. J. Electrochem. Sci*., 10 (2015) 6935.
22. L. Ichim, M. Prodana and C. Dumitriu, *UPB Sci Bull Ser. B.*, 78 (2016) 161.
23. F. Mansfeld, *Corrosion*, 29 (1973) 397.
24. L. Ichim, B. G. Sbarcea, D. Patroi and C. Dumitriu, *Rev.Chim.*, 67 (2016) 2198.
25. J. M. Parnis and K. B.Oldham, *J. Photochem*., 267 (2013) 6.

© 2018 The Authors. Published by ESG (www.electrochemsci.org). This article is an open access article distributed under the terms and conditions of the Creative Commons Attribution license (http://creativecommons.org/licenses/by/4.0/).